

Analysis of Spectral Indices of Images Captured from an Unmanned Aerial Vehicle at the ANA Moyocancha Altitude Station

W, Oñate

Escuela Superior Politécnica de Chimborazo (ESPOCH), Dirección postal 060106

P Vaca

Investigador externo FCPPI. 202, ESPOCH, Dirección postal 060106

M Moscoso

Escuela Superior Politécnica de Chimborazo (ESPOCH), Dirección postal 060106

M.Vaca-Cárdenas

Escuela Superior Politécnica de Chimborazo (ESPOCH), Dirección postal 060106

Abstract

This research analyzed vegetation cover through the application of the vegetation index transition matrix (NDVI-GNDVI) at the Aña Moyocancha High Altitude Station using aerial images captured by drone. The images were captured using the Sendera-Sensor AGX710 multispectral camera and the DJI M200 remotely piloted aerial vehicle; the DJI Pilot application was used for flight planning. Subsequently, the images were processed in Pix4Dmapper software. Once the spectral bands were generated, they were entered into ArcGIS 10.8 software to calculate the indices; these were reclassified, transformed and the intersection matrix was applied. The results obtained showed a maximum NDVI value of 1 and a minimum of -0.9991, for the GNDVI a maximum value of 1 and a minimum of -0.9991, the reclassification determined for the NDVI the middle class with 108.2 representing 51.28 %, followed by the high class with 38.58 Ha. covering 38.58% and the low class represented 21.4 Ha, The middle class represented 137 ha (65.03 %), followed by the low class with 72.13 ha (20%) and the high class with 1.66 ha (0.79 %). It is concluded that the analysis using the intersection tool identified eight categories. The low coincidence category covered an area of 1.65 ha, which established spaces with infrastructure, the medium coincidence category covered 0.000737 ha, which determined areas of sparse vegetation and the high coincidence category with 0.113067 ha corresponded to shrub vegetation.

Keywords: *Remote sensing, spectral indices, NDVI, GNVI, herbaceous moorland, transition matrix.*

1. INTRODUCTION

In recent years, a large loss of wetlands has been estimated globally, with South America as the second most affected region, with a loss of 32% of these ecosystems [1]. Among the wetlands of the South American region are the high Andean wetlands, which are located along the Andes in the páramo, jalca and puna ecosystems [2]. Although international organizations such as the Ramsar Convention

catalogued high Andean wetlands as strategic ecosystems for the region in 2002 [3], these ecosystems are still under great threat and vulnerability due to two predominant variables: the agricultural frontier expansion and climate change [4].

Remote sensing consists of studying the vegetation of a scene from reflectivity measurements independently of all the factors that disturb the radiometric signal, among

which the reflectivity of the soil is one of the most important. The application of remote sensing is possible thanks to the interaction of electromagnetic energy with land covers that have a variable reflective behavior, conditioned by their state at the time of image acquisition [5]. Furthermore, measuring reflectance with optical sensors has the potential to provide information on the status of different crops [6].

Vegetation indices are images calculated from algebraic operations between different spectral bands. The result allows for a new image where certain pixels related to plant cover parameters are graphically highlighted: density, leaf area index and chlorophyll activity. The Normalized Difference Vegetation Index (NDVI) has been widely used as an indicator of plant biomass vigor in studies related to crop performance and natural forest vegetation. However, this index has many modifications to correct certain deficiencies [7]. The NDVI index ranges between -1 and 1, whose values lower than 0.1 are interpreted as bare soils or water bodies. Higher values are equivalent to the vegetation cover; the higher the values indicate the photosynthetic activity of the various coverages (shrublands, temperate forest, jungle and agricultural activity) [8, 9].

The spectral index Green Normalized Difference Vegetation Index (GNDVI), defined by Gitelson et al. (1996), was calculated to show the range of greenness of plant leaves or photosynthetic activity. It is one of the most widely used indexes in vegetation analysis to determine the uptake of water and nitrogen in the layer of branches and leaves. In identifying different chlorophyll concentration rates, GNDVI is more effective than NDVI in identifying different chlorophyll concentration rates, as it is highly correlated with nitrogen in plants [10,11,12]. The values yielded by the NDVI also range from -1 to 1. Values between -1 and 0 are associated with water or bare soil. This index is mainly used in the intermediate and final stages of the crop cycle; it is a variant

of NDVI that uses the green band instead of the red band [13].

Uncrewed aerial vehicles (UAS/RPAS) have been developed recently as a new versatile platform for acquiring small images with many applications in cartography, thermography and agriculture [14]. Concerning this last aspect, spectral images and the utility of uncrewed aerial vehicles have allowed a better characterization of what happens in the crop through vegetation indices [15]. Vegetation indices, or green indices, are transformations that involve performing a mathematical combination between the digital levels stored in two or more spectral bands of the same image [16], making it possible to estimate the quantity, quality and development of the crop. Moreover, specific wavelengths of this spectrum are absorbed when sunlight strikes objects, and others are reflected [17].

The processing of aerial images captured by RPAS is performed in the PIX4D software, developed in 2011, with the main function of creating high-precision georeferenced 2D and 3D digital models and maps from drone images. The software recognizes the type of camera and the geographic reference system; the processing is divided into three sections: photo alignment, point cloud generation and generation of orthomosaic and spectral indices [18,19].

Despite the multiple benefits provided by the moorlands, they are very vulnerable to ecological imbalance generated by direct human actions such as deforestation, changes in land use and grazing, and indirect actions such as the increase in global temperature due to climate change, which in the end is a consequence linked to the bad practices that society manages. With this background, it is necessary to carry out a study of the vegetation index information (NDVI, GNDVI) for the generation of a conservation and recovery program of the existing flora, thus ensuring the sustainability of the páramo ecosystem, since it

is characterized by having a large amount of biomass, which can capture energy, store it and transfer nutrients to the grazing chains, thus ensuring an adequate transfer of nutrients from the plant to the soil system, thus improving the biotic and abiotic conditions of the ecosystem.

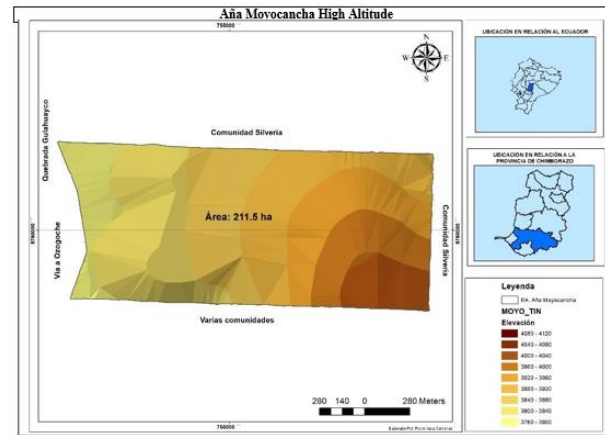
This research aimed to analyze the vegetation cover through the application of the transition matrix (NDVI) and the green normalized difference vegetation index (GNDVI) at the Altura Aña Moyocancha station using aerial images and to determine the current state of vegetation cover.

2. Materials and methods

Study area

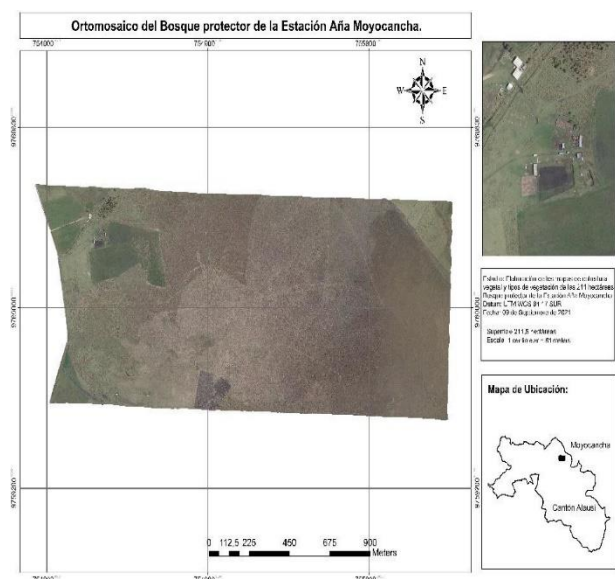
The study was carried out in the “Aña Moyocancha” High Altitude Station at the “Escuela Superior Politécnica de Chimborazo” located 85 km from the city of Riobamba, in the Tixán parish belonging to the Alausí canton, specifically between the communities of Silveria Santa Lucia and the Ozogоче lagoons. The investigation was part of the research project “Floristic Inventory of the Protected Forest of the High Altitude Station “Aña Moyocancha”, which lasted 18 months. The area’s temperature is around 80 C., with a relative humidity of 92%, and rainfall of 1000 mm and altitude ranges from 3800 to 4200 meters above sea level.

Figure 1. Map of the study area - Aña Moyocancha Station.



This ecosystem corresponds to the herbaceous paramo (Sierra et al. 1999). The vegetation is composed of eight families (Poaceae, Cyperaceae, Asteraceae, Haloragaceae, Rosaceae, Plantaginaceae, Apiaceae and Fabaceae) and 27 species, including grasses such as *Calamagrostis vicunarum*, *Paspalum pygmaeum* and *Paspalum bonplandianum*, *Calamagrostis intermedia*, *Anthoxanthum odoratum*, *Mulhbergia ligularis*, *Festuca dolicophylla*, and *Agrostis breviculmis*, among others.

Figure 2. Orthomosaic- Aña Moyocancha Station



Evaluation methodology

This research has a quantitative approach in that the data are numerical. It is field research at a descriptive, analytical and prospective level. It was carried out through bibliographic reviews using inductive and deductive methods. The equipment used in this research was a DJI M200 commercial drone, a Sendera multispectral camera - AGX710 sensor, computer, Trimble Juno 3b handheld GPS - sub-meter precision receiver and Motorola communication radios.

First, the site was georeferenced in UTM WGS 84 17 SOUTH geographic coordinates, and the surface of the study area was quantified and labeled. Next, the data were processed with a GIS tool. Then, the state and vegetation type were recognized through a review of secondary sources.

The Sendera AGX710 multispectral camera, equipped with a 12.3MP BSI CMOS sensor, captured aerial images. This camera allows the capture of still images: JPEG and video: MP4, captures data in 12.3MP Stills, 4K Ultra HD video at 30 fps 1080p / 720p Video [20], is compatible with the DJI M200 remotely piloted aerial vehicle (RPAS). The RPAS is considered an industrial drone that provides exceptional information through plug-and-play technology, allowing it to capture data quickly, develop high-precision spectral index measurements, and run deep learning algorithms [21].

Before the generation of the flight mission, the climatic variables that may interfere during the execution of the flight are investigated and analyzed. For example, the presence of high-speed wind, humidity, rain and extreme temperatures can affect the performance of UAVs; the presence of wind alters the trajectory of the UAV, affecting its control and decreasing the flight time, thus increasing the battery consumption; the physical components of the aircraft can be affected by extreme temperatures that limit its aerodynamic

performance, influencing the density and performance of the UAV.

Finally, humidity would affect the electronic equipment inducing it to lose communication and control of the aircraft.

In this regard, the available data on wind, humidity and temperature in the study area were investigated from historical records of the National Institute of Meteorology and Hydrology (IMANHI) and the “mountain-forecas” website, obtaining data on precipitation, temperature, wind speed and cloudiness [22,23].

To plan the flight, the DJI Pilot application was used at an altitude of 80 meters, capturing images with a pixel resolution of 30 cm/pixel, with an overlap of 80% and a lateral overlap of 70%, with a flight duration of approximately four hours. To cover the study area, 7 flights were developed, all at a speed of 8 m/s, with 200 control points, reaching flights of between 35 and 40 minutes per set of batteries, managing to capture 4340 photographs for the 211 ha of the study area. The flights were made between 11:30 and 13:00 hours to obtain better results because, during this time of the day, there is greater photosynthetic activity due to greater incident solar radiation.

The images taken during the flight were transferred from the camera to a computer and then processed in the Pix4Dmapper Ag software. This software has been widely used in precision agriculture and topography applications [24,25,26]. In addition, it allows converting thousands of 2D images into georeferenced mosaics, accurate 3D models, point clouds, elevation models, and different files in (*.TIFF) format with each index to be calculated. Also, PIX4D contains the most common and default indexes.

The processing starts when the images are loaded into the Pix4D software, which recognizes the type of multispectral camera used and the geographic reference system,

which in this case was UTM WGS 84 17 SOUTH. Subsequently, the photo-alignment process is executed, the cloud points are generated, and finally, the DSM, Orthomosaic and spectral indices are obtained [27].

Once the spectral bands were available, they were entered into the GIS software using the “Raster Calculator” tool that allows creating and executing a map algebra expression that generates a raster as output [28] for calculating the spectral indices.

For the analysis and monitoring of vegetative conditions and their dynamics in the land cover, the NDVI spectral index was calculated, which is derived through the response of the vegetation to the electromagnetic spectrum, being expressed as indicated by the following equation [29,30].

Formula applied in the raster calculator = $(\text{NIR} - \text{Red}) / (\text{NIR} + \text{Red})$, where NIR is near-infrared light, and Red is visible red light.

To show the range of greenness of the plant leaves or photosynthetic activity, the spectral index GNDVI was calculated, which allows for determining the uptake of water and nitrogen in the layer of branches and leaves. The formula of the spectral index GNDVI corresponds to:

The formula applied in the raster calculator: $\text{Float “NI”} - \text{“GREE”} / \text{Float “NI”} + \text{“GREE”}$

Reclassification of the two spectral indices into medium, high and low values was performed using the “Reclassify” tool, which reclassifies or changes the values in a raster. Then, this raster was transformed into vectors using the “Raster to Polygon Conversion” tool that converts a raster dataset into polygon entities [28].

The coincidences between indices were analyzed using the transitional matrix, which is the starting point for land cover analysis and land use change patterns [31]. This method relates two data sources from maps [32]. First,

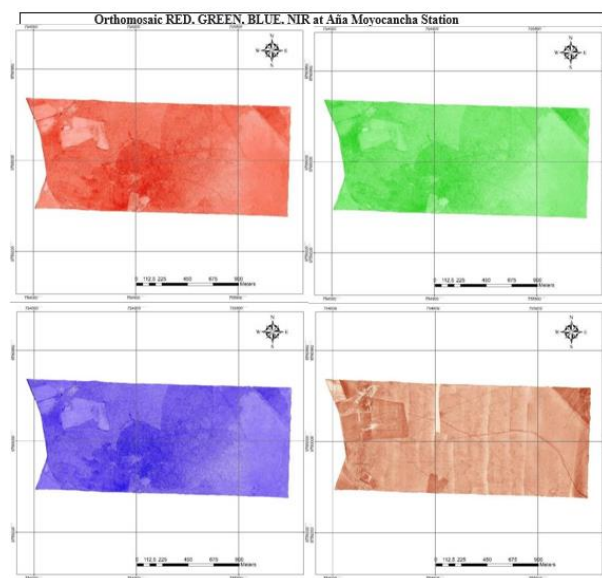
they are described as tables with symmetrical arrangements containing in the rows figures of vegetation and land use for some time or of a specific nature and in the columns these same elements, but of another period or type. Each cell of the main diagonal of such a matrix represents the area in hectares of each vegetation cover and land use class that remained in the same category, while the rest of the cells estimate the area of a particular cover or land use type that moved to another category [33], which allows understanding the dynamics of change in land cover and land use.

The transition matrix allowed for generating a table from the intersection that determines similarity and change rates for each vector layer [34]. The matrix is composed of rows corresponding to the NDVI vector layer with the high mean and low values, and in the column, the reclassified values of the GNDVI were placed [35]. The areas that coincide with the classes of each index are shown in the main diagonal of the table, while the elements outside the main diagonal belong to the relationships between the categories of the two spectral indices [36]. The process was performed with the “Intersec” tool that calculates a geometric intersection of the input entities. Entities or parts of entities that overlap in all layers and entity classes are written to the output entity class.

3. Results and Discussion

Once the aerial images were processed in the PIX 4dMapper software, the following bands were obtained:

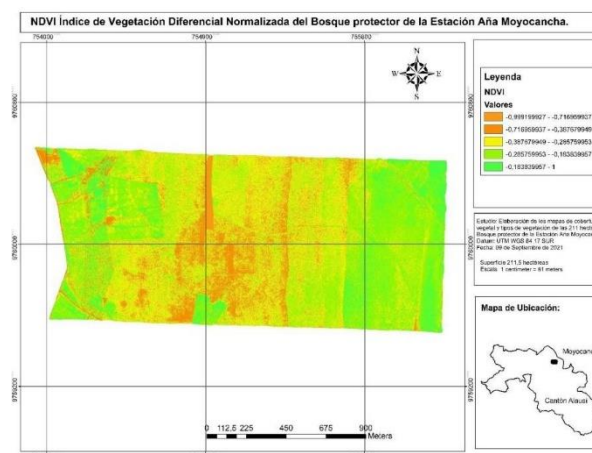
Figure 3. Maps of the RED, GREEN, BLUE, NIR Orthomosaic at Aña Moyocancha Station.



Map 1 shows the RED band Orthomosaic, which allows determining chlorophyll uptake, thus very useful for land cover, agriculture and land use classification; Map 2 represents the GREEN band Orthomosaic, designed to assess the vigor of healthy vegetation, differentiate rock types and measure water quality; Map 3 presents the BLUE band Orthomosaic, helpful in mapping water bodies, differentiating between soil and vegetation, differentiating between coniferous and deciduous vegetation; and Map 4 displays the NIR band Orthomosaic that models the part of the spectrum reflecting from healthy plants.

Once the NDVI formula was applied, the following map (Figure 4) was obtained for the Aña Moyochancha station.

Figure 4. Map of the NDVI index at Aña Moyocancha Station.



It was determined that at the Aña Moyocancha high altitude station, the maximum NDVI value is 1, concentrated mainly in the eastern flank zone, decreasing towards the central part and reappearing in several sections of the western and southern part of the study area; the average NDVI value is 0.13, concentrated in the central section of the study area and the minimum NDVI value is -0.9991, concentrated in sections that go from the western flank towards the central zone of the station. The variation in the intensity of the vegetation coloration is presented: intense green when the NDVI is higher, yellow when the NDVI has medium values and orange when the NDVI has low values.

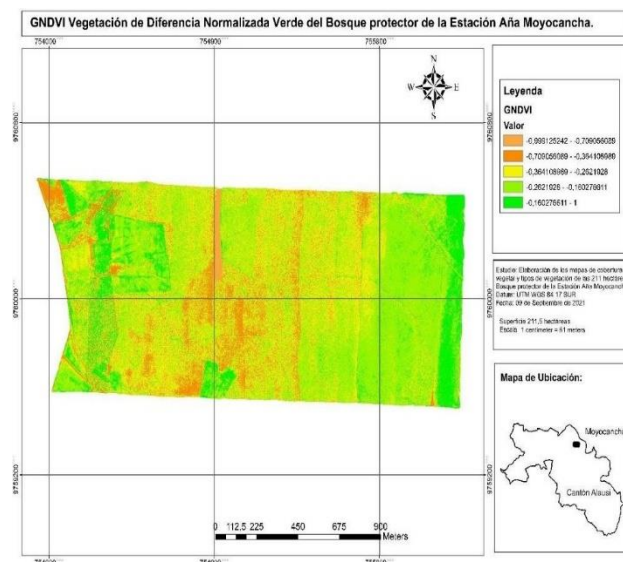
Values similar to those found in the study “Evaluation of the state of the Puglllohuma wetland, belonging to the Antisana water conservation area (Acha), through the analysis of spectral indices of images captured from an unmanned aircraft (UAV)” where a minimum value of -0.03 is presented, with the highest number of pixels from the value 0.26 and with a lower number of pixels reaching a maximum value of 0.95 of the NDVI spectral index [37]. Results comparable to those reviewed in the study “Analysis of multispectral images acquired with unmanned aerial vehicle” in sugarcane plantations where 0.2 is reported as

the minimum value and 0.5 as the maximum value [38]. And those reported by the study Estimation of pasture yield using NDVI with imagery multispectral unmanned aerial vehicle (UAV” exposing a minimum value of 0.34 and a maximum value of 0.59 [39].

It can be noted that the vegetation cover presents significant variations in response to various land use factors; the study area is composed mainly of herbaceous vegetation, having a high reflectance in the near-infrared, facilitating its estimation.

Subsequently, the GNDVI spectral index calculation map was obtained for the Aña Moyocancha station, applying the formula previously described.

Figure 5. Map of the GNDVI index at the Aña Moyocancha station.



It was determined that at the Aña Moyocancha station, the maximum value of GNDVI is 1, which is mainly concentrated in the section of the eastern flank, decreases towards the central part and reappears in a section of the western and southern part of the study area; the average value of GNDVI is 0.15, which is concentrated in the central section of the study area and the minimum value of GNDVI is -0.9991, which is concentrated in the section that goes from the western flank towards the central part of the study area. Map 6 shows the variation of the vegetation color intensity, being intense green when the GNDVI is higher, yellow when the GNDVI has medium values and orange when the GNDVI has low values.

Values are comparable to those reported in the study entitled “Evaluation of the state of the Puglllohuma wetland, belonging to the Antisana (Acha) water conservation area, through the analysis of spectral indices of images captured from an unmanned aircraft (UAV)” where a minimum value of 0.00 minimum is presented, without showing negative values and with a maximum value of 0.9 of the GNDVI spectral index [36]. This data differs from that presented in the study “Analysis of aerial images as a support for the monitoring of pasture crops for cattle consumption,” in which all the data are positive, with a minimum value of 0.25 and a maximum value of 0.82 of the GNDVI spectral index [40].

The reclassification of the NDVI and GNDVI spectral indices allowed to distinguish 3 intervals with values detailed in the following table:

Table 1. Intervals of the reclassification of the spectral indices

Intervals	GNDVI values	NDVI values
1	from -0.999125 to -0.671144	from -0.9992 to -0.413497
2	from -0.671144 to 0.1	from -0.413497 to 0.1
3	from 0.1 to 1	from 0.1 to 1

Class 1 represents areas with lower values that correspond to areas without vegetation due to the existence of infrastructure and roads mainly; class 2 represents areas with medium values that correspond to areas with sparse vegetation that may be due to trampling and grazing; and class 3 represents areas with higher values that correspond to areas with dense vegetation.

Figure 6. Reclassified NDVI and GNDVI maps of the Aña Moyocancha station.

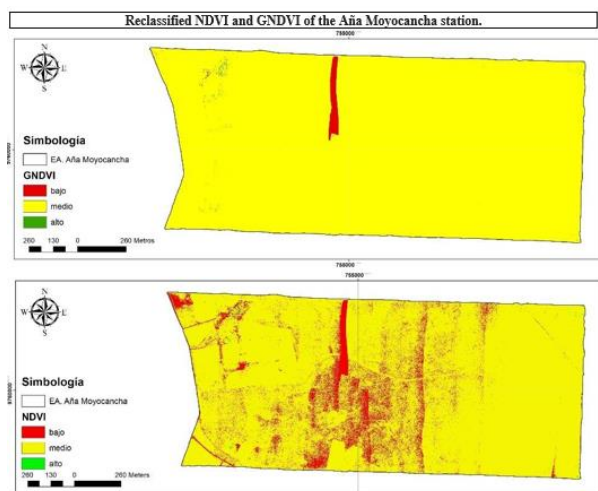


Figure 6) shows the reclassified NDVI spectral index map, exposing that the largest area is in the middle class with 108.2 ha, occupying 51.28 %, followed by the high class with 38.58 ha covering 38.58%, while the low class would represent 21.4 ha occupying 1.14 %. In addition, Figure 7 presents the map of the reclassified GNDVI spectral index, showing that the largest area is in the middle class, with

137 ha occupying 65.03 %, followed by the low class with 72.13 ha occupying 20%, while the high class would represent 1.66 ha occupying 0.79 % of the station area.

The analysis using the intersection tool between the NDVI and GNDVI indices shows eight categories represented in the following map (Figure 7).

Figure 7. Intersection between the reclassified NDVI and GNDVI indices.

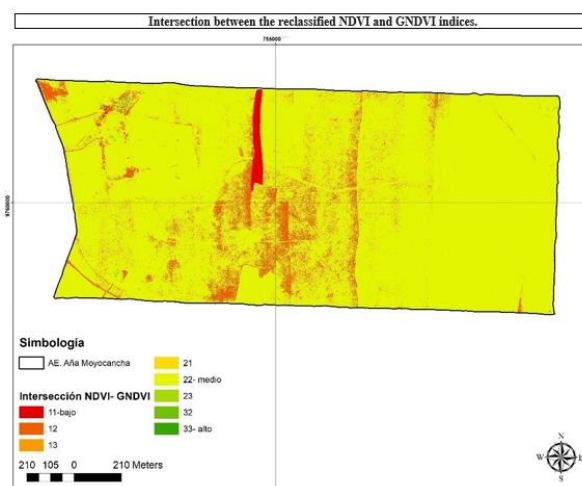


Figure 8 shows the match categories with value 11 for the low level with a red coloration, a yellowish coloration for value 22 representing the medium level match and for the high-level match with coding of 33 with a dark green coloration.

Table 2. Transition matrix of NDVI and GNDVI spectral indices.

Transition matrix ha		Low NDVI		Average NDVI		High NDVI	
		10		20		30	
GNDVI low	1	1.655339	11	0.000043	21	0.043074	31
GNDVI medium	2	19.628954	12	0.000737	22	0.041988	32
GNDVI high	3	0.000043	13	189.975039	23	0.113067	33

The coincidences of the low categories of the GNDVI and NDVI spectral indices cover an

area of 1.65 ha that determine areas with infrastructure; the coincidences of the medium

category of the two spectral indices cover an area of 0.000737 ha that determine areas of sparse vegetation, possibly subjected to trampling; the coincidence of the high category covers an area of 0.113067 ha corresponding to shrub vegetation. The most significant number of pixels that coincide between the two indices are those of the low category, followed by the high category and finally, those of the medium category.

Code 12 (medium GNDVI - low NDVI ratio) corresponds to 19.62 ha and indicates areas without vegetation - roads. Code 13 (high GNDVI - low NDVI ratio) corresponds to 0.000043 ha and indicates that there are areas with sparse vegetation - fences, code 21 (low GNDVI - medium NDVI) corresponds to 0.000043 ha and indicates that there are areas with sparse vegetation - fences, code 21 (low GNDVI - medium NDVI) corresponds to 0.000043 ha and indicates that there are code 23 (high GNDVI ratio and medium NDVI) occupies most of the area, indicating that there is an area of 189.9 ha with medium dense vegetation; code 31 (low GNDVI ratio and high NDVI) is an area of 0.043074 ha corresponding to areas with dense vegetation and code 32 (medium GNDVI ratio and high NDVI) has an area of 0.041988 ha, corresponding to areas with shrub vegetation.

4. Conclusions

Drones have recently been used as an environmental remote sensing system and represent an excellent tool for high-precision monitoring and analysis. In the present study, they have made it possible to obtain 4340 images of areas with a resolution of 30 cm/pixel, with flights at an altitude of 80 meters, making it easier to identify problems and take measurements in large areas with limited access and in a shorter work time.

The intersection analysis of the NDVI and GNDVI spectral indices coincides with the detection of moderately dense vegetation,

identifying areas with regular photosynthetic activity.

The use of the GNDVI spectral index is recommended for vegetation analysis as it is evidenced that it has better detection of high categories. Consequently, it provides a better view of biomass.

Reference

- [1]. Hu, S., Niu, Z., Chen, Y., Li, L., & Zhang, H. (2017). Global wetlands: Potential distribution, wetland loss, and status. *Science of the Total Environment*, 586, 319–327.
<https://doi.org/10.1016/j.scitotenv.2017.02.001>
- [2]. WWF, W. W. F. G. D. (2005). Los humedales altoandinos. Retrieved from http://awsassets.panda.org/downloads/los_humedales_altoandinos_es.pdf
- [3]. Secretaría de la Convención de Ramsar. (2002). Ramsar COP8 Resolución VIII.39. Retrieved from http://archive.ramsar.org/pdf/res/key_res_viii_39_s.pdf.
- [4]. Orúe, M. E., Laterra, P., & Cabria, F. (2007). Expansión de la frontera agrícola en Argentina y erosión hídrica: mapas de riesgo utilizando el Modelo Usle con apoyo de SIG. Congreso de La Asociación Española de Teledetección, 185–145 192. Retrieved from <http://www.aet.org.es/congresos/xii/arg24.pdf>
- [5]. Pérez, C y Muñoz, A. Teledetección nociones y aplicaciones. Universidad de salamanca. 356 p. ISBN-10: 84-611- 1613-5. 2006.
- [6]. Giletto, CM; Silva, SE; Cassino, MN; Zamuner, EC; Echeverria, HE. 2016. Caracterización del estrés de nitrógeno en papa para industria usando el NDVI = Characterizing nitrogen stress in

- processing potato using NDVI (Consulta:12/07/2022). Asociación Argentina de la Ciencia del Suelo. <https://explore.openaire.eu/search/publication?articleId=od3056:40616c7ffd72ba53c5>.
- [7]. Gonzaga C (2015), Aplicación de índices de vegetación derivados de imágenes satelitales para análisis de coberturas vegetales en la provincia de Loja, Ecuador. CEDAMAZ, ISSN 1390-5880, Vol 5.
- [8] Yengoh, G. T., Dent, D., Olsson, L., Tengberg, A. E., & Tucker III, C. J. (2015). Use of the Normalized Difference Vegetation Index (NDVI) to assess Land degradation at multiple scales: current status, future trends, and practical considerations. Springer.
- [9] Van Leeuwen, W. J., Hartfield, K., Miranda, M., & Meza, F. J. (2013). Trends and ENSO/AAO driven variability in NDVI derived productivity and phenology alongside the Andes Mountains. *Remote Sensing*, 5(3), 1177-1203.
- [10] Gitelson, A. A., Kaufman, Y. J., & Merzlyak, M. N. (1996). Use of a green channel in remote sensing of global vegetation from EOS-MODIS. *Remote sensing of Environment*, 58(3), 289-298.
- [11] Kemerer, A., Di Bella, C., Melchiori, R., Benech, A., & Alvarez, R. (2007). Comparación de índices espectrales para la predicción del IAF en canopeos de maíz. In XII Congreso de Teledetección Google Scholar
- [12] Kharuf-Gutierrez, S., Orozco-Morales, R., Díaz, O. D. L. C. A., & Ruiz, E. P. (2018). Multispectral aerial image processing system for precision agriculture. *Sistemas y Telemática*, 16(47).
- [13] Moreno-García, B., Casterad, M. A., Guillén, M., & Quílez, D. (2018). Agronomic and economic potential of vegetation indices for rice N recommendations under organic and mineral fertilization in Mediterranean regions. *Remote Sensing*, 10(12), 1908.
- [14] Díaz, G., & Cervigón, J. (2015). Estudio de índices de vegetación a partir de imágenes aéreas tomadas desde UAS/RPAS y aplicaciones de estos a la agricultura de precisión. Universidad Complutense de Madrid, Facultad de Geografía e Historia.
- [15]. Stanley Best (INIA), Agricultura de precisión. Accesibilidad al usuario INIA Chile -Instituto de Investigaciones Agropecuarias, Chile; 2012.
- [16] Esperanza, F., & Zerda, H. Potencialidad de los índices de vegetación Para la discriminación de coberturas forestales. Universidad Nacional de Santiago del Estero, Facultad de Ciencias Forestales, Santiago del Estero; 2002.
- [17] Costales Acurio, G. A. Análisis comparativo entre los software de prueba Agisoft Photoscan y Pix4D para el procesamiento de datos obtenidos con fotogrametría de vehículo aéreo no tripulado (UAV) de bajo costo aplicado a proyectos de medio ambiente, Bachelor's thesis, Quito; 2018.
- [18] Pix4D. (2020). Pix4D Documentation. Disponible en: <https://support.pix4d.com/hc/en-us/articles/202558539-Input-files#label1>
- [19] Teran, M., & Viteri, L. Procesamiento de imágenes satelitales para determinación de cambios de cobertura vegetal y deforestación utilizando Matlab (tesis de grado). Escuela Politécnica Nacional, Quito, Ecuador; 2005
- [20] El vuelo del dron. Cámara Sentera AGX710. El vuelo del dron. 2020 [citado el 29 de julio del 2022]. Disponible en:

- [http://
https://elvuelodeldrone.com/repuestos-y-
accesorios/camara-drone-
profesional/camara-dual-sentera-agx710-
rgb-nvdi/](http://https://elvuelodeldrone.com/repuestos-y-accesorios/camara-drone-profesional/camara-dual-sentera-agx710-rgb-nvdi/)
- [21] GARCÍA-CERVIGÓN, Díaz; JOSÉ, Juan. Estudio de índices de vegetación a partir de imágenes aéreas tomadas desde UAS/RPAS y aplicaciones de éstos a la agricultura de precisión. 2015.
- [22] Sauter, B. Weather Impacts on the Aerostar Unmanned Aircraft System Based on Climatology over the U.S./Mexico Border. 2007.
- [23] Ranquist, E., Steiner, M., & Argrow, B. Exploring the Range of Weather Impacts on UAS Operations. 18th Conference on Aviation, Range and Aerospace Meteorologia; 2016.
- [24] Romero VR, Villareal AM, León JLT, Hernández AH. Perspectivas de la tecnología VANT en el cultivo de palma de aceite: monitorización del cultivo mediante imágenes aéreas de alta resolución. Revista Palmas. 2015;36(3):25-41.
- [25] Gago J, Douthe C, Coopman R, Gallego P, Ribas-Carbo M, Flexas J, et al. UAVs challenge to assess water stress for sustainable agriculture. Agricultural Water Management. 2015; 153:9-19.
- [26] Suh J, Choi Y. Mapping hazardous mining-induced sinkhole subsidence using unmanned aerial vehicle (drone) photogrammetry. Environmental Earth Sciences. 2017;76(4):144.
- [27] ArcGIS (s,f). ArcGIS® software by Esri. ArcGIS® and ArcMap™ are the intellectual property of Esri and are used herein under license. Copyright © Esri. All rights reserved. For more information about Esri® software, please visit www.esri.com. 2020.
- [28] Rouse Jr, J. W., Haas, R. H., Schell, J. A., & Deering, D. W. (1973). Monitoring the vernal advancement and retrogradation (green wave effect) of natural vegetation (No. NASA-CR-132982).
- [29] Pix4D. (2020b). Menu Process > Processing Options... > 1. Initial Processing > General – Support. Retrieved March 15, 2020, from [https://support.pix4d.com/hc/en-
us/articles/202557759-Menu-
ProcessProcessing-Options-1-Initial-
Processing-General#label3](https://support.pix4d.com/hc/en-us/articles/202557759-Menu-ProcessProcessing-Options-1-Initial-Processing-General#label3)
- [30] Kundu, A., Denis, D. M., Patel, N. R., & Dutta, D. (2018). A Geo - spatial study for analysing temporal responses of NDVI to rainfall. Singapore Journal of Tropical Geography, 39(1), 107-116.
- [31] Camacho Sanabria, J. M., Pérez, J. I. J., Pineda Jaimes, N. B., Cadena Vargas, E. G., Bravo Peña, L. C., & Sánchez López, M. (2015). Cambios de cobertura/uso del suelo en una porción de la Zona de Transición Mexicana de Montaña. Madera y Bosques, 21(1), 93–112. <https://doi.org/10.21829/myb.2015.211435>
- [32] Rojas Briceño, N. B., Barboza Castillo, E., Maicelo Quintana, J. L., Oliva Cruz, S. M., & Salas López, R. (2019). Deforestación en la Amazonía peruana: índices de cambios de cobertura y uso del suelo basado en SIG. Boletín de La Asociación de Geógrafos Españoles, 81, 1–34. <https://doi.org/10.21138/bage.2538a>
- [33] Pontius, R., Shusas, E., & McEachern, M. (2004). Detecting important categorical land changes while accounting for persistence. Agriculture, Ecosystems & Environment, V. 101, 251-268.

- [34] Gallardo, M., & Martinez, V. J. (2012). Cambios de usos del suelo en la comunidad de Madrid: analizando el pasado y simulando el futuro. XV Congreso Nacional de Tecnologías de la Información Geográfica. Madrid.
- [35], López, G. E. M.; Bocco, G. y Mendoza, C. M. E. 2001. Predicción del cambio de cobertura y uso del suelo. El caso de la ciudad de Morelia. Investigaciones Geográficas, Boletín del Instituto de Geografía-Universidad Nacional Autónoma de México (UNAM). 45(1):56-76
- [36] Niño Martinez, Y. M. N. (2020). Análisis Multitemporal Mediante Imágenes De Sensores Remotos Para La Determinación De Los Cambios De Uso De Suelo En El Municipio De San Francisco De Sales, Cundinamarca (Colombia) Entre Los Años 90'S Y 2018" [Universidad Nacional de La Plata]. In Angewandte Chemie International Edition, 6(11), 951–952.
- [37] PALMA CASTRO, Kevin Alejandro. Evaluación del estado del humedal Pugllolhuma, perteneciente al área de conservación hídrica Antisana (ACHA), mediante el análisis de índices espectrales de imágenes capturadas desde una aeronave no tripulada (UAV). 2020. Tesis de Licenciatura. Quito, 2020.
- [38] KHARUF-GUTIERREZ, Samy, et al. Análisis de imágenes multiespectrales adquiridas con vehículos aéreos no tripulados. Ingeniería Electrónica, Automática y Comunicaciones, 2018, vol. 39, no 2, p. 79-91.
- [39] GONZALEZ, IZAR SINDE, et al. (2020) Estimación del rendimiento del pasto mediante NDVI calculado a partir de imágenes multiespectrales de vehículos aéreos no tripulados (UAV). Revista Geoespacial, vol. 17, no 1, p. 25-38.
- [40] CRISTANCHO TOLOZA (2020) Cristian Hernando. Análisis de imágenes aéreas como apoyo para el seguimiento de cultivos de pasto para consumo bovino.